RSC Advances

PAPER

View Article Online
View Journal | View Issue

Cite this: *RSC Adv.*, 2022, **12**, 19528

Determination of aflatoxin B1 in *Pixian Douban* based on aptamer magnetic solid-phase extraction†

Chaoyi Zeng,‡[ad] Chi Xu,‡[a] Hongyun Tian,[c] Kun Shao,[a] Yaning Song,[a] Xiao Yang,[a] Zhenming Che[ab] and Yukun Huang *[ab]

Aflatoxin B1 (AFB_1) is considered as the most prevalent and toxic mycotoxin in food, and is the indispensable index in the monitoring of *Pixian Douban*, a traditional chinese fermented bean paste from Sichuan. However, the effeciency of AFB_1 detection in *Pixian Douban* is influenced by the traditional extraction, which is usually complex and time consuming. Therefore, an aptamer-based magnetic solid-phase extraction method was designed for the pretreatment of AFB_1 in this sample, for which Fe_3O_4 was synthesized *via* the solvothermal method and then a Fe_3O_4@SiO_2–NH_2 with a core–shell structure was prepared, followed by an AFB_1-aptamer attachment. The validation was performed *via* an enzyme-linked immunosorbent assay and compared with HPLC-MS/MS. The linearity range of this method was 0.5–2.0 ng mL $^{-1}$ with R^2 of 0.981, and recoveries of AFB_1 ranged from 80.19% to 113.92% with RSDs below 7.28% with no significant differences compared to HPLC-MS/MS. The three-time reusability efficiencies of aptamer-MNPs were averaged at 78.24%. The results proved that aptamer-MNPs were high-performance adsorbents for extracting and enriching AFB_1, facilitating quick and effective detection of AFB_1 in *Pixian DouBan* samples.

Received 1st May 2022
Accepted 30th June 2022

DOI: 10.1039/d2ra02763a

rsc.li/rsc-advances

1. Introduction

Pixian Douban is a fermented condiment with chinese regional characteristics. Its fermentation was recorded to be accompanied with a process called "sun and night dew" treatment. The complex changes of temperature to a certain extent can affect the various *Aspergillus* and enzymes that play a biochemical role, and form unique flavour characteristics widely used in Sichuan Cuisine. However, due to the relatively extensive process of traditional production, *Douban's* fermentation is liable to be contaminated by other *Aspergillus* and subsequently cause aflatoxin pollution.[1,2] The evidence shows that AFB_1 has the highest pollution frequency in this food.[3] It has been reported that AFB_1 can lead to liver cancer and other diseases in mammals,[2,4] which is classified as type I carcinogen by international cancer research institutions.[1,5] In order to reduce food safety risk of *Pixian Douban*, AFB_1 has been regarded as a necessary item in *Pixian Douban's* Geographical Indication Product Standard of GB/T 20560-2006. Traditional detection methods mainly include thin layer chromatography, high performance liquid chromatography, gas chromatography, capillary electrophoresis and immunoassay.[3,6,7] Generally speaking, these detection methods are relatively wide-applied in the practical detection right now. However, the broad bean is rich in nutrients such as protein, amino acids, enzymes, pigments, lipids and other components,[8] which is too complex to be easily detected with high efficiency so far. The shortcomings of traditional detection methods, such as long detection time, high detection cost and poor repeatability as well as not environment friendly, pose great challenges to the effective monitoring of AFB_1 in *Douban*. Therefore, it is necessary to establish an efficient, simple, and robust method for detection of AFB_1 in *Pixian Douban*.

Methanol solvent extraction is adopted in the commercial ELISA kit method, which is a solid–liquid extraction for AFB_1. Then a quantitative analysis can be performed according to the colour depth after coloration. However, the blending of chilli in *Pixian Douban* brings bright red colouring matter into the extract, which shows the background interference in ELISA determination. Aptamers have several advantages, such as strong specificity, high affinity, wide target range, *in vitro* chemical synthesis, low molecular weight, and good stability. As

[a]*School of Food and Biological Engineering, Chongqing Key Laboratory of Speciality Food Co-Built by Sichuan and Chongqing, Xihua University, Chengdu 610039, China. E-mail: hyk_diana@163.com*

[b]*Key Laboratory of Food Non Thermal Processing, Engineering Technology Research Center of Food Non Thermal Processing, Yibin Xihua University Research Institute, Yibin 644004, China*

[c]*Shandong Institute of Food and Drug Control, Jinan 250101, China*

[d]*Department of Food Biotechnology, Faculty of Biotechnology, Assumption University, Bangkok 10240, Thailand*

† Electronic supplementary information (ESI) available. See https://doi.org/10.1039/d2ra02763a

‡ The authors contributed equally in this work.

a result, aptamers have been widely used in the fields of analytical chemistry, medicine, environmental monitoring, and food safety control.[9–12] In addition, magnetic solid-phase extraction (MSPE) is a new solid-phase extraction (SPE) method based on the use of magnetic adsorbents, in which suitable adsorbents are combined with magnetic materials.[13,14] In the MSPE method, magnetic adsorbents are critical for the efficient enrichment of analytes. Ferrosoferric oxide (Fe_3O_4) is widely used in sample pretreatment because of its characteristics of magnetic adsorption, low price, easy synthesis, and surface modification.[15–17] Nevertheless, Fe_3O_4 is unstable and easily oxidized by air. Surface modification of Fe_3O_4 with appropriate functional groups can prevent oxidation and improve its durability and adsorption.[13] The modification and functionalization of Fe_3O_4 are conducted mainly by using graphene,[18] graphene oxide,[19] carbon quantum dots,[20] the polymer,[21] and so on. Silica is one of the best coating materials for Fe_3O_4 magnetic nanoparticles (MNPs), because it owns characteristics of easy surface modification, high chemical stability, and environmental compatibility.[17,22] Currently, aptamer-Fe_3O_4-based composite adsorption materials are gradually applied to various samples pretreatments, such as metal elements,[23] bacteria,[21,24] pesticides,[25] veterinary drug,[26] toxins,[27] nucleotides,[28] and other samples. Recently, the extraction method of AFB_1 from dairy products and edible vegetable oils,[29–31] such as SPE and MSPE, have been extensively studied in a fast, simple, inexpensive and safe method.

The deep eutectic solvent–based matrix solid-phase dispersion (DES-MSPD) method has currently been established for extracting and enriching aflatoxins (AFB_1, AFB_2, AFG_1, and AFG_2) in various crops.[32] A simple modified SPE combined with high-performance liquid chromatography (HPLC)-fluorescence detection was established for detecting AFB_1 and AFB_2, and amine-functionalized MNPs were successfully employed in SPE for the first time for adsorbing AFB_1 and AFB_2 in drugs[33] In addition, aptasensors are considered as an emerging strategy for quantifying AFB_1 with high selectivity and sensitivity.[34]

In this work, the functionalization of Fe_3O_4@SiO_2–NH_2 using ssDNA aptamers (referred to as aptamer-MNPs) was designed to prepare AFB1-specific nanoparticles with excellent magnetic responses. Moreover, various adsorption conditions were tested to determine the optimal conditions for the adsorption of AFB_1 in *Pixian Douban* to the prepared nanomaterials. The variables tested included the amount of aptamer-MNPs, extraction time, elution time, elution types, and elution volumes. An efficient method for extracting AFB_1 from *Pixian Douban* was established, which lays the foundation for the subsequent analysis of AFB_1 in food.

2. Materials and methods

2.1. Materials and reagents

The main text of the article should appear here with headings as appropriate. Ferric chloride hexahydrate ($FeCl_3 \cdot 6H_2O$) and AFB_1 standard were purchased from Shanghai Yuanye Biological Co., Ltd. (Shanghai, China). Poly (4-styrenesulfonic acid-co-maleic acid) sodium salt (PSSMA) was purchased from Huaxia Reagent Co., Ltd. (Harbin, China). Tetraethyl silicate (TEOS), 3-aminopropyltriethoxysilane (APTES), and glutaraldehyde were purchased from Shanghai McLean Company (Shanghai, China). The AFB_1 kit was purchased from Jiangsu Suwei Co., Ltd. (Jiangsu, China). Hydroxymethylaminomethane (Tris) and streptavidin were purchased from Shanghai Shenggong Co., Ltd. *Pixian Douban* was purchased from the local supermarket. Biotinylated aptamer (5′-GT TGG GCA CGT GTT GTC TCT CTG TGT CTC GTG CCC TTC GCT AGG CCC ACA-Biotin-3′) was synthesized by Shanghai Shenggong Bioengineering Co., Ltd. (Shanghai, China). Further, NaAc, NaOH, ethanol, $NH_3 \cdot H_2O$, KCl, $CaCl_2$ were purchased from Cologne Chemicals Co., Ltd. (Chengdu, China).

2.2. Methods

The preparation of aptamer-MNPs comprises two steps: the preparation of Fe_3O_4@SiO_2–NH_2 nanoparticles and the functionalization of AFB_1-aptamer, as shown in Scheme 1a.

2.2.1. Preparation of Fe_3O_4@SiO_2–NH_2 nanoparticles

2.2.1.1. Preparation of Fe_3O_4 nanoparticles. The preparation method for Fe_3O_4 nanoparticles reported by previous researchers[35] was slightly modified. 1.08 g of $FeCl_3 \cdot 6H_2O$, 3.0 g of NaAc, and 1.2 g of PSSMA were added in 40 mL of ethylene glycol. The mixture was uniformly stirred in an oil bath at 50 °C. Then, 0.6 g of NaOH was added to the mixture and continuously stirred until the solution became dark. Subsequently, the mixture was transferred to a stainless-steel autoclave, and Fe_3O_4 nanoparticles were obtained after being heated at 190 °C for 9 h. Fe_3O_4 nanoparticles were uniformly dispersed in 30 mL of distilled water (Fe_3O_4 concentration was approximately 0.8 wt%) and stored at 4 °C.

2.2.1.2. Preparation of Fe_3O_4 @SiO_2. 12 mL of dispersion were dispersed in 70 mL of ethanol and transferred to a round-bottomed flask. After stirring for 15 min, 0.4 mL of TEOS and 4 mL of $NH_3 \cdot H_2O$ were added twice at 20 min intervals into the reaction mixture. Subsequently, Fe_3O_4@SiO_2 nanoparticles were obtained after stirring for 80 min.

2.2.1.3. Preparation of Fe_3O_4 @SiO_2–NH_2. 50 mg of Fe_3O_4@SiO_2, 6 mL of distilled water, and 40 mL of anhydrous ethanol were added into the flask for ultrasonic dispersion. Then, 3 mL of ammonia was added to the mixture and stirred for 15 min. Furthermore, 10 mL of anhydrous ethanol and 2 mL of the APTES mixture were added and stirred for 10 h to obtain Fe_3O_4@SiO_2–NH_2. The upper liquid was discarded by magnetic separation, washed using PBS (2.7 mmol L^{-1} of KCl, 137 mmol L^{-1} of NaCl, 2 mmol L^{-1} of KH_2PO_4 and 10 mmol L^{-1} of Na_2HPO_4, and pH = 7.4) thrice, dispersed in 10 mL of PBS, and stored at 4 °C.

2.2.2. AFB_1-aptamer functionalization. 20 mL of PBS, 40 mg of Fe_3O_4@SiO_2–NH_2, and 5 mL of 25% glutaraldehyde-water solution were subjected to oscillation reaction at 110 r per min for 2 h. The reaction solution was removed *via* magnetic separation. After washing with PBS, it was dispersed in 16 mL of PBS (containing 960 μg streptavidin) and was subjected to oscillation for 12 h. After conducting magnetic separation and discarding the reaction solution, washing three times with PBS

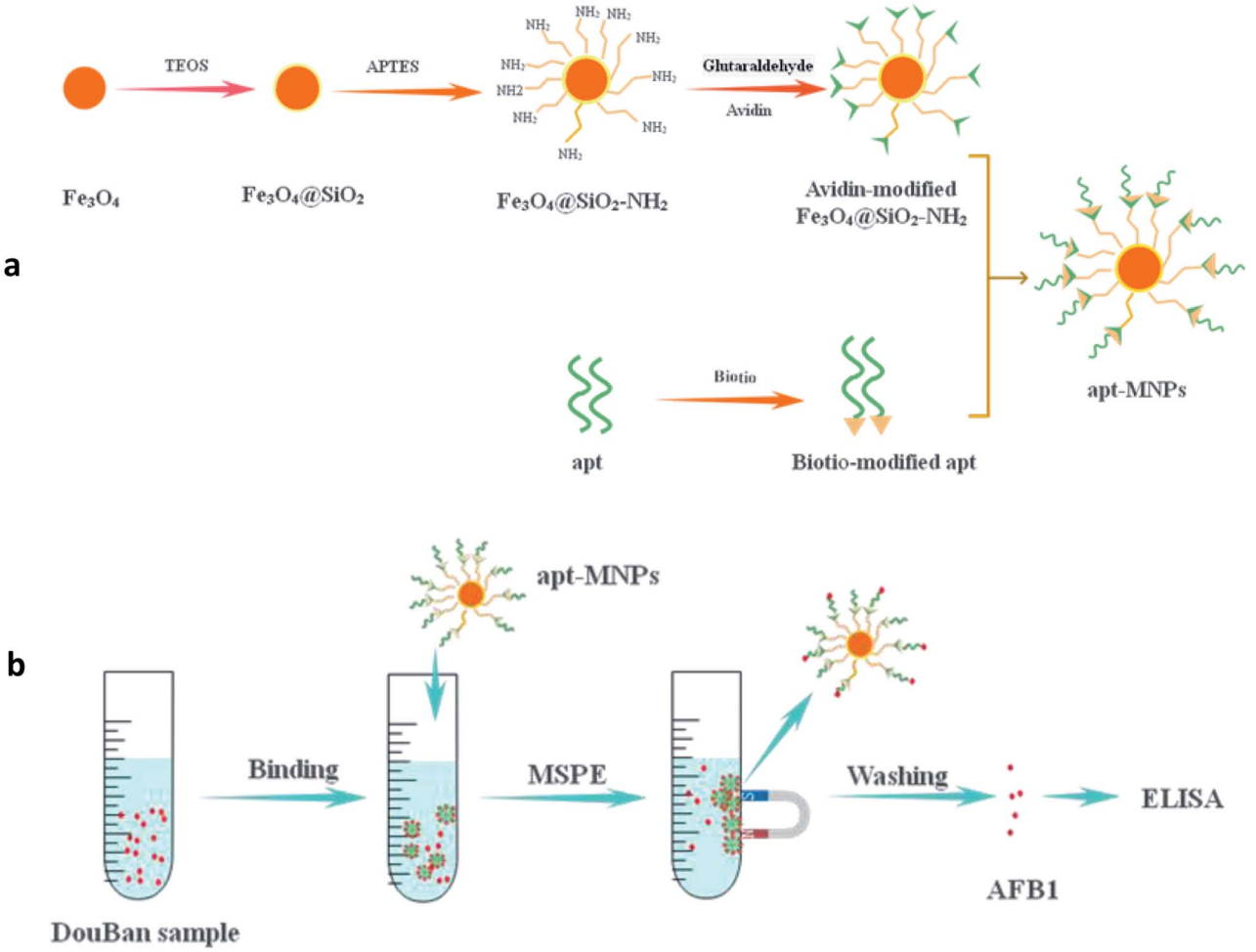

Scheme 1 Schematic illustration of the synthesis process of aptamer-MNPs nanocomposite (a); a schematic diagram for the extraction and detection of AFB1 in *Pixian Douban* samples (b).

and dispersed in 20 mL of PBS to obtain avidin-modified nanomagnetic beads. 40 mg of avidin magnetic beads were dispersed in 40 mL of PBS (containing an AFB_1-aptamer concentration of 400 pmol ml^{-1}) and oscillated at 28 °C for 2 h. Aptamer-MNPs were obtained *via* magnetic separation and stored in 40 mL of Tris–HCl (10 mM of Tris, 120 mM of NaCl, 5 mM of KCl, 20 mM of $CaCl_2$, and pH = 8.5).

2.2.3. Characterization of synthesized nanomaterials. The synthesized nanomaterials were characterized *via* particle size analyzer, transmission electron microscopy (TEM), Fourier transform infrared spectroscopy (FT–IR), X-ray diffraction (XRD), and UV-visible (UV-Vis) spectrophotometer.

2.2.4. Extraction and detection of AFB_1. A new method for detecting AFB_1 in *Pixian Douban* was developed using aptamer-MNPs adsorbents along with ELISA (Scheme 1b).

2.2.4.1. Aptamer-MNPs extraction of AFB_1. 10.0 g of *Pixian Douban,* 50 ml of 50% aqueous methanol solution, and 20 mL of n-hexane were subjected to oscillation for 15 min and transferred to the separator funnel to stratify the solution. 10 mL of the solution at the lower layer was collected and concentrated *via* rotary evaporation. 10% of methanol-Tris-HCl was added to redissolve and obtain a crude sample extract. After 1 mL of crude extract and 5 mg of aptamer-MNPs were incubated with shaking for 30 min, the aptamer-MNPs were separated using a magnet. The separated aptamer-MNPs were washed with Tris–HCl, and 1 mL was eluted with methanol for 10 min. The eluate was collected and concentrated to near dryness, and then redissolved in 1 mL of PBS solution. 50 μL of the solution was used for ELISA.

2.2.4.2. Detection of AFB_1 by ELISA. 200 μL of detergent was added to each hole of the ELISA plate. After 1 min, the detergent was shake off and patted dry. Repeat the washing plate once. In each well, 50 μL of the standard solution or sample solution, and 50 μL of enzyme-labeled antigen solution were added, shaken and mixed well, incubated for 30 min at 37 °C, the detergent was shaken off the reaction solution, and patted dry. 200 μL of detergent was added and placed for 2 min, patted dry and repeat the washing plate for four times. 50 μL of the chromogenic substrate a and 50 μL of chromogenic substrate b were added, shaken and mixed, incubated at 37 °C for 15 min, and 50 μL of terminating solution was added. After shaking well, the absorbance at a wavelength of 450 nm was determined *via* ELISA.

2.2.4.3. Comparison detection of AFB_1 by HPLC-MS/MS. HPLC-MS/MS analysis was compared to the present work as the way of replacing ELISA test in the spike recovery of *Pixian Douban* samples. After Aptamer-MNPs treatment, the extractive was redissolved with acetonitrile-water (60 + 40 *v*/*v*). HPLC-MS/MS system (Agilent 6460) detection conditions:[38] AFB_1 were chromatographed on ACQUITY BEH-18 column (1.7 μm particle size, 110 × 2.1 mm i. d., waters) and separated using gradient elution with 2 mmol L^{-1} ammonium acetate aqueous solution and acetonitrile as mobile phase A and B, respectively (both acidified with 0.2% formic acid). The gradient program was as follows: at time zero 10% solvent B; at 2 min 35% solvent B; linear gradient to 60% solvent B within 7 min, at 9 min 90% solvent B then 10% B isocratic for 3 min. The flow rate was 0.3 mL min^{-1}. The ionization was carried out with an ESI interface in positive mode as follows: spray capillary voltage was 4.0 kV; sheath gas flow rate 11 L min^{-1}, respectively; temperature of sheath gas 350 °C. The mass spectrometric analysis was performed in MRM. For fragmentation of AFB_1 $[M + H]^+$ ions is 313 *m*/*z*., the detected and quantified fragment ions were: 241 and 269 *m*/*z* for AFB_1. Quantitative determination was performed by MassHunter software (Agilent). All analyses were performed with the SPSS 23.0 software (SPSS Incorporated, USA). Statistical significance was analyzed using ANOVA. In all statistical comparisons, values of $P \leq 0.05$ were considered as of significance, and values of $P \leq 0.01$ were considered to be markedly significant.

3. Results and discussion

3.1. Characterization

3.1.1. Characterization of nanometer magnetic beads by Fe_3O_4, Fe_3O_4@SiO_2, and Fe_3O_4@SiO_2–NH_2. TEM images (Fig. S1†) and Fig. S2† show that the prepared Fe_3O_4 were regular spheres, with a particle size of 20–50 nm, and mainly concentrated around 35 nm. This shows that the prepared Fe_3O_4@SiO_2 particles were regular spheres. It had a clear core–shell structure, and the thickness of the SiO_2 shell was approximately 15 nm. The presence of Fe_3O_4@SiO_2 afforded a quite different morphology (Fig. S1a and S1b†). It can be seen that Fe_3O_4@SiO_2 had a homogeneous cover layer on the surface, which can be attributed to the successful coating of SiO_2 on Fe_3O_4. The addition of PSSMA during the preparation of Fe_3O_4 can negatively charge the surface of the magnetic beads, increase the stability of the Ostwald ripening process, and allow Fe_3O_4 to uniformly grow and stably disperse in the solution.[35] In addition, SiO_2-modified Fe_3O_4 has better dispersibility.

The XRD pattern of Fe_3O_4 samples is shown in Fig. S3.† The XRD spectra of Fe_3O_4 show spinel ferrites, which fully matches with the diffraction card JCPDS (PDF-#76-1849). The diffraction peaks at $2\theta = 18.06°$, 30.13°, 35.47°, 43.03°, 53.19°, 56.89°, and 62.58°, corresponding to 111, 220, 311, 400, 422, 511, and 440 plates, respectively, indicate a magnetic phase and the crystalline cubic spinel structure of Fe_3O_4.[23]

The magnetic separation of Fe_3O_4@SiO_2 from deionized water was performed to test the practical magnetic responseability (Fig. S4†). Fe_3O_4@SiO_2 particles were uniformly dispersed in deionized water. Under the presence of magnetic field, Fe_3O_4@SiO_2 was rapidly separated from the solution and assembled in the corner near the magnet.

The FT-IR spectra of Fe_3O_4 and Fe_3O_4@SiO_2–NH_2 are depicted in Fig. S5.† The absorption peak at 3381.39 cm^{-1} was attributed to the stretching vibration of the hydroxyl group, indicating that a certain number of hydroxyl groups exist on the surface of Fe_3O_4. In the FT-IR spectra of Fe_3O_4@SiO_2–NH_2, the absorption intensity of the Fe–O group decreased with the addition of silica. The Si–O–Si group exhibited a strong absorption intensity at 1100.21 cm^{-1} owing to the silica coating, indicating that Fe_3O_4 had been successfully coated with SiO_2.[36] In addition, the Absorption peaks at 1627.94 and 3328.89 cm^{-1} correspond to bending and stretching vibrations of the–NH_2 group,[16] respectively. The peaks at 2856.35 and 2923.24 cm^{-1} correspond to symmetric and asymmetric stretching vibrations of the –CH_2 group, respectively, which are attributed to the hydrolysis of the amination reagent APTES. These absorption peaks confirmed the successful modification of Fe_3O_4. The absorption peaks at 588.63 and 583.22 cm^{-1} are attributed to the characteristic absorption peak of the Fe–O group. After the surface modification of Fe_3O_4, the characteristic absorption peak slightly shifted, but the properties of Fe_3O_4 did not change.

3.1.2. Characterization of avidinized Fe_3O_4 @ SiO_2–NH_2 and aptamer-MNPs. In this experiment, Fe_3O_4@SiO_2–NH_2 of avidin magnetic beads and aptamer-MNPs were characterized *via* the ultraviolet absorption of avidin at 280 nm and aptamer at 260 nm. Fig. S6a† shows that the absorbance at 280 nm considerably decreased, which indicated that the content of avidin in the solution decreased. The avidin covalently bound to glutaraldehyde and was connected to the surface of magnetic beads. In addition, the experiment continued to explore the relationship between dosage of magnetic beads and concentration of avidin. The experimental results show that when 1 mg of magnetic beads (Fe_3O_4@SiO_2–NH_2) were incubated with 24 μg of avidin, and almost all the avidin is coupled to the surface of the magnetic beads to attain saturation. The absorbance value at 260 nm considerably decreased (Fig. S6b†), indicating a decrease with the concentration of aptamer decreasing. Aptamer bound to the surface of avidin magnetic beads. In addition, the experiment was continued to investigate the aptamer-MNPs binding ability, and the results showed that the aptamer concentrated on the surface of 1 mg avidin magnetic beads (Fe_3O_4@SiO_2–NH_2) attained saturation after being incubated with 400 pmol of aptamer.

3.2. The establishment of detection standard curve

In this experiment, a commercial AFB_1 ELISA kit was used for performing the quantitative analysis of AFB_1 extracted using aptamer-MNPs. The standard curve of ELISA was obtained after step 2.2.4.2. As shown in Fig. 1, the linearity of the developed method was observed over a range of 0.5–2.0 ng mL^{-1}, with a correlation coefficient of 0.981.

3.3. Optimization of sample preparation conditions

In the MSPE procedure, the extraction and elution processes are crucial in realizing satisfactory recovery of analytes. To obtain

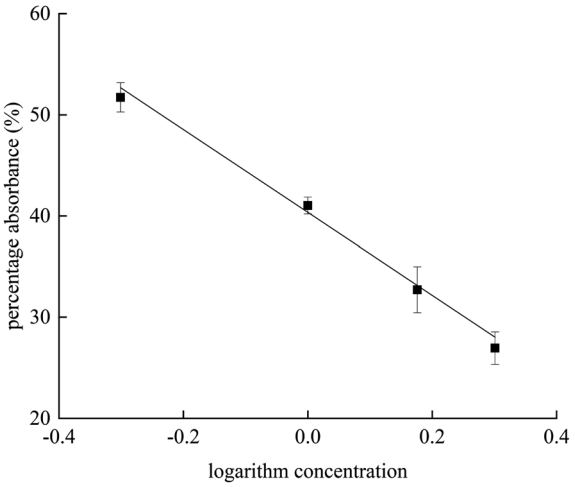

Fig. 1 Standard curve of AFB_1.

higher extraction recoveries, AFB_1 in *Pixian Douban* was enriched with aptamer-MNPs. The main experimental parameters that affect the recovery of the extraction were optimized, such as the amount of aptamer-MNPs, extraction time, and elution time of the sample.

3.3.1. The influence of the amount of aptamer-MNPs on AFB_1 recoveries. The amount of magnetic adsorbent is crucial in realizing satisfactory recoveries of the target analytes.[13] Fig. 2. Shows that the AFB_1 recoveries varied with the amount of aptamer-MNPs. The dosage of adsorbents is proportional to the adsorption rate within a certain range. The larger the dosage of magnetic adsorbents, the more active sites on the surfaces of the adsorbents.[13,37] With increasing the amount of aptamer-MNPs from 3 mg to 5 mg, the recovery of AFB_1 gradually increased. The recovery of AFB_1 did not considerably increase as the number of magnetic beads increased but decreased slightly. The low AFB_1 recovery rate at 6 mg may be attributed to the experimental operation error. Finally, 5 mg is determined to be the optimum amount of aptamer-MNPs to ensure the good recovery of each compound and is used in subsequent experiments.

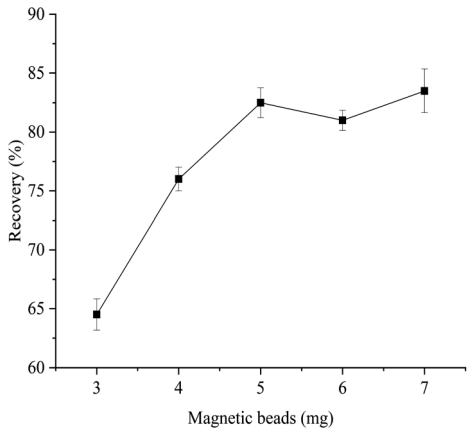

Fig. 2 The effect of aptamer-MNPs amount on the recovery of AFB_1 ($n = 3$).

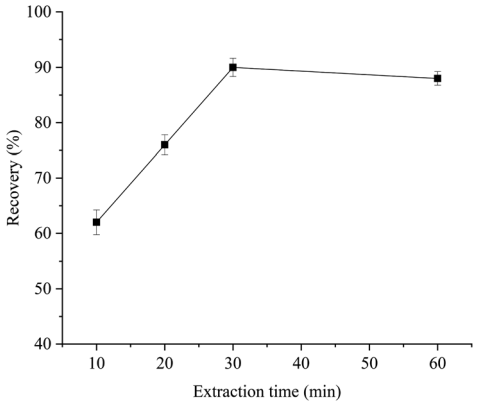

Fig. 3 The effect of extraction time on the recovery of AFB_1 ($n = 3$).

3.3.2. The influence of extraction time on AFB_1 recoveries. Adsorption is an equilibrium process, and sufficient contact time between the sample solutions and sorbents should be provided to establish the extraction equilibrium.[37] Therefore, the binding of aptamer-MNPs to AFB_1 under different extraction times was investigated in this experiment. As shown in Fig. 3, with increasing the extraction time, the adsorption capacity of AFB_1-MNPs to AFB_1 increased gradually. When the extraction time increased to 30 min, the extraction efficiency of AFB_1 by aptamer-MNPs was the highest. When the extraction time was prolonged, the recovery rate of AFB_1 decreased gradually, which indicated that when the extraction time was 30 min, the aptamer's recognition and capture of AFB_1 had attained a saturated state.

3.3.3. The influence of the desorption time on AFB_1 recoveries. In this study, methanol was used to elute AFB_1 from aptamer-MNPs and the effect of different desorption times on the recovery rate was investigated Fig. 4 shows that the recovery rate decreases with increasing the desorption time and the best recovery rate is obtained when the elution time is 5 min.

3.3.4. The influence of other factors on AFB_1 recoveries. In this experiment, the influence of the types of solvents was investigated in addition to optimizing the three key factors

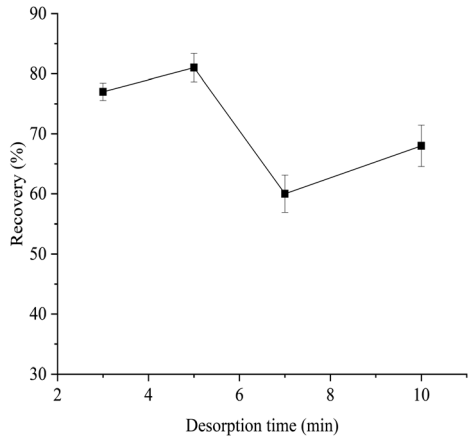

Fig. 4 The effect of desorption time on the recovery of AFB_1 ($n = 3$).

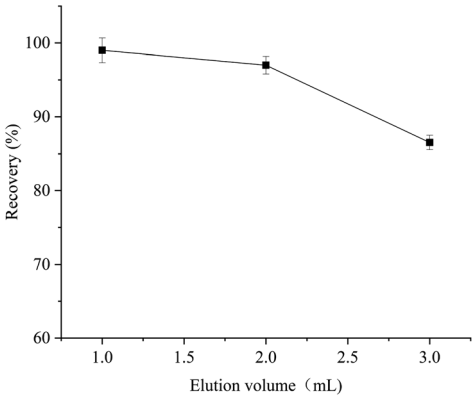

Fig. 5 The effect of the elution volume on the recovery of AFB_1 ($n = 3$).

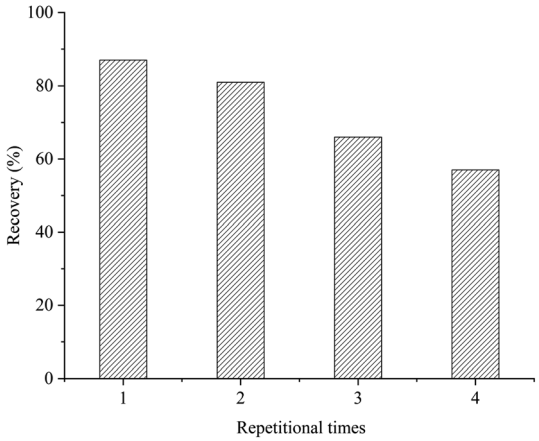

Fig. 6 Reusability in four cycles of the aptamer-MNPs SPME adsorbents for extraction of AFB_1 in *Pixian Douban* samples.

affecting extraction efficiency. The experiment compared two types of elution solvents: methanol and acetonitrile. The two elution solvents had almost similar influence on the recoveries of AFB_1, indicating that both methanol and acetonitrile could be used as elution solvents. Considering the cost and toxicity of the reagent, methanol was chosen as the elution solvent. In addition, this study also explored the effects of different volumes of elution (1 and 3 mL) on the recoveries of AFB_1 (Fig. 5). Compared with 1 mL of methanol solution, 3 mL of methanol solution may cause a greater loss in the process of volatilization and redissolution after elution reducing the extraction efficiency. Therefore, the experiment decided to use 1 mL of methanol solution.

3.4. Method performance validation

3.4.1. Spike recovery experiment. The AFB_1 content in the samples determined by using ELISA was 3.4 μg kg^{-1}, less than the national standard limit of 5.0 μg kg^{-1}. AFB_1 was spiked into *Pixian Douban* samples at concentrations of 0.5 μg L^{-1}, 1.0 μg L^{-1}, 2.0 μg L^{-1}, and 10.0 μg L^{-1}, and the experiment was performed according to step 2.2.4.1. A comparative evaluation of the spiked samples was performed by using the present method and HPLC-MS/MS, respective. Qualitative identification was conducted by using MRM scan in HPLC-MS/MS method shown in Fig. S7b and c;† then the linear regression analysis was carried out in Fig. S7a.† The recoveries and the corresponding RSDs were presented in Table 1. The recoveries of proposed measurement of AFB_1 ranged from 80.19% to 113.92% with RSDs lower than 7.28% ($n = 3$), while those of the compared HPLC-MS/MS were 88.63% to 101.10% with RSDs below 3.44% ($n = 3$). The P values of the test concentrations of the two methods were 0.259, 0.365, 0.432 and 0.452 respectively, which were all greater than 0.05($P > 0.05$), indicating that there was no significant statistical difference between the methods. Thus, the extraction method is efficient and feasible.

3.4.2. The reusability of aptamer-MNPs. The reusability of the material was investigated based on the recovery as an index, and the result is depicted in Fig. 6. The reusability of the selected membrane for aptamer-MNPs indicated efficiencies of 87.34%, 81.20%, 66.17%, and 57.02% for the 1st, 2nd, 3rd, and 4th cycles, respectively. The results show that the aptamer-MNPs prepared using this method exhibit reusability when used in the MSPE for detecting AFB_1.

Compared with traditional SPE, MSPE affords enhanced extraction efficiencies and avoids time-consuming and labor-intensive extraction steps, which are particularly important when considering large sample sets.[13] Table 2 shows a comparison of sample preparation procedures with other methods in the literature. The LOD and LOQ obtained from the present method are comparable to or lower than those obtained from other methods. The MSPE method simplifies the sample preparation procedure because the adsorption processes are fast and the magnetic adsorbents can be easily separated from the sample solution under the applied external magnetic field.[30] The MSPE method established in this study can identify target molecules with high specificity and realize rapid separation and enrichment under an external magnetic field, which saves the operation of centrifugation and filtration in other extraction methods, greatly simplifying the experimental steps, and reducing the experiment

Table 1 Recoveries of AFB_1 in spiked sample by compared methods ($n = 3$)

Tagged value/(ng mL^{-1})	ELISA Detected value/(ng mL^{-1})	Recovery/(%)	RSD/(%)	HPLC-MS/MS Detected value/(ng mL^{-1})	Recovery/(%)	RSD/(%)
0.5	0.42	84.29	3.27	0.44	88.63	1.37
1.0	1.14	113.92	7.28	0.89	89.88	2.91
2.0	1.60	80.19	2.34	1.87	93.50	1.32
10.0	9.37	93.70	2.30	10.11	101.10	3.44

Table 2 Comparison of sample preparation procedures and LOQs with different methods[a]

Method/(ng mL^{-1})	Sample	Adsorbent	LOD (ng mL^{-1})	LOQ (ng mL^{-1})	Linear range (ng mL^{-1})	Ref.
MSPE-aptamer-ELISA	*Pixian Douban*	Aptamer@Fe_3O_4@SiO_2–NH_2	0.17	0.48	0.5–2	Present work
ELISA	*Pixian Douban*	—	0.41	1.26	0.5–2	Comparison 1
MSPE-aptamer-HPLC-MS/MS	*Pixian Douban*	Aptamer@Fe_3O_4@SiO_2–NH_2	0.07	0.22	0.5–10	Comparison 2
MSPE-UHPLC	Milk	PEG-MWCNTs-MNP	0.01	0.03	1.25–40	30
MSPE-HPLC	Vegetable oils	PDA@Fe_3O_4-MWCNTs	0.20	0.60	1–50	31
MSPD-HPLC	Crops	TBAC-hexyl alcohol DES	0.10	0.33	0.1–100	32

[a] Note: "-" means the sample preparation procedures without aptamer@Fe_3O_4@SiO_2–NH_2.

time. In addition, aptamer has strong chemical stability and storage stability; therefore, it can be used in various reaction systems and can be preserved for a long time without any reduction in its functional activity. Aptamer and nanomagnetic beads have the advantages of simple preparation, easy modification, and good stability.[39] Therefore, the specific recognition of aptamer and the rapid separation as well as enrichment of nanomagnetic beads are integrated to prepare a new type of extraction material, and the pretreatment method for the detection of AFB_1 is demonstrated to have great significance and value.

Conclusions

In this study, aptamer-MNPs were prepared and adopted as the adsorbents for AFB_1 in *Pixian Douban* samples. Aptamer-MNPs effective in extracting and enriching the targeted compound AFB_1 and exhibited a good magnetic response. A new detection method for AFB_1 in *Pixian Douban* samples was developed by combining aptamer-MNPs with ELISA. The linearity of the method was 0.5–2 ng mL^{-1} with a correlation coefficient of 0.981, and the content of detections for AFB_1 was 3.4 μg kg^{-1}. The recoveries of AFB_1 ranged from 80.19% to 113.92% with RSDs lower than 7.28%, and the reusability of the selected membrane for aptamer-MNPs indicated efficiency of 87.34%, 81.20%, and 66.17% for the 1st, 2nd, and 3rd cycles, respectively. The results proved that aptamer-MNPs were high-performance adsorbents for extracting and enriching AFB_1, which can quickly and effectively detect AFB_1 in *Pixian Douban* samples.

Author contributions

All authors contributed to the study conception and design. Material preparation, data collection, analysis, and revision were performed by Chi Xu, Kun Shao, Yaning Song and Hongyun Tian. The first draft of the manuscript was written by Chaoyi Zeng and the previous versions of the manuscript were commented by Xiao Yang. The resources and supervision were provided by Zhenming Che. The conceptualization and writing – review and editing were done by Yukun Huang. All authors read and approved the final manuscript.

Conflicts of interest

There are no conflicts to declare.

Acknowledgements

This work was partly supported by the National Natural Science Foundation of China (31801647), Sichuan Science and Technology Program (2020YFN0153, 2020YFN0151, 2022JDTD0028), Research project of Sichuan Cuisine Development research Center (CC22Z27).

References

1 A. Vaz, A. C. Cabral Silva, P. Rodrigues and A. Venâncio, Detection Methods for Aflatoxin M1 in Dairy Products, *Microorganisms*, 2020, **8**, 246.
2 O. Ketney, A. Santini and S. Oancea, Recent aflatoxin survey data in milk and milk products: A review, *Int. J. Dairy Technol.*, 2017, **70**, 320–331.
3 L. Zhang, W. Xu, P. Yue, Q. Wang, Y. Li, X. Pei and P. Zeng, High occurrence of aflatoxin B1 in Pixian Doubanjiang, a typical condiment in chinese cuisine, *Food Control*, 2020, **110**, 107034.
4 A. C Manetta, *Aflatoxins: Their Measure and Analysis*, InTech, 2011.
5 M. Heinrich, IARC Monographs on the Evaluation of Carcinogenic Risks to Humans: Some Traditional Herbal Medicines, Some Mycotoxins, Naphthalene and Styrene, *J. Ethnopharmacol.*, 2002, **88**, 299–300.
6 N. W. Turner, S. Subrahmanyam and S. A. Piletsky, Analytical methods for determination of mycotoxins: A review, *Anal. Chim. Acta*, 2009, **632**, 168–180.
7 P. Li, Z. Zhang, X. Hu and Q. Zhang, Advanced hyphenated chromatographic-mass spectrometry in mycotoxin determination: Current status and prospects, *Mass Spectrom. Rev.*, 2013, **32**, 420–452.
8 Y. Huang, Y. Song, F. Chen, Z. J. Jiang, Z. M. Che, X. Yang and X. G. Chen, Simultaneous determination of eight biogenic amines in the traditional Chinese condiment Pixian Douban using UHPLC-MS/MS, *Food Chemistry*, 2021, **353**, 129423.
9 Z. Lu, X. Chen and W. Hu, A fluorescence aptasensor based on semiconductor quantum dots and MoS_2 nanosheets for ochratoxin A detection, *Sens. Actuators, B*, 2017, **246**, 61–67.
10 S. Zhang, L. Ma, K. Ma, B. Xu, L. Liu and W. Tian, Label-Free Aptamer-Based Biosensor for Specific Detection of Chloramphenicol Using AIE Probe and Graphene Oxide, *ACS Omega*, 2018, **3**, 12886–12892.

11 S. Kim and H. J. Lee, Gold Nanostar Enhanced Surface Plasmon Resonance Detection of an Antibiotic at Attomolar Concentrations *via* an Aptamer-Antibody Sandwich Assay, *Anal. Chem.*, 2017, **89**, 6624–6630.

12 H. Gao, N. Gan, D. Pan, Y. Chen, T. Li, Y. Cao and T. Fu, A sensitive colorimetric aptasensor for chloramphenicol detection in fish and pork based on the amplification of a nano-peroxidase-polymer, *Anal. Methods*, 2015, **7**, 6528–6536.

13 Z. Liu, P. Qi, J. Wang, Z. Wang, S. Di, H. Xu, H. Zhao, Q. Wang, X. Wang, and X. Wang, *Development, validation, comparison, and implementation of a highly efficient and effective method using magnetic solid-phase extraction with hydrophilic-lipophilic-balanced materials for LC-MS/MS analysis of pesticides in seawater*, Science of the Total Environment, 2020, p. 708.

14 L. Kubíčková, J. Koktan, T. Kořínková, M. Klementova, T. Kmjec, J. Kohout, A. Weidenkaff and O. Kaman, Zn-substituted iron oxide nanoparticles from thermal decomposition and their thermally treated derivatives for magnetic solid-phase extraction, *J. Magn. Magn. Mater.*, 2020, 498.

15 Z. Liu, P. Qi, X. Wang, Z. Wang, X. Xu, W. Chen, L. Wu, H. Zhang, Q. Wang and X. Wang, Multi-pesticides residue analysis of grains using modified magnetic nanoparticle adsorbent for facile and efficient cleanup, *Food Chemistry*, 2017, **230**, 423–431.

16 Z. Yuan, R. Xu, J. Li, Y. Chen, B. Wu, J. Feng and Z. Chen, Biological responses to core-shell-structured Fe_3O_4@SiO_2-NH_2 nanoparticles in rats by a nuclear magnetic resonance-based metabonomic strategy, *Int. J. Nanomed.*, 2018, **13**, 2447–2462.

17 J. Li, Z. Yuan, H. Liu, J. Feng and Z. Chen, Size-dependent tissue-specific biological effects of core–shell structured Fe_3O_4@SiO_2–NH_2 nanoparticles, *J. Nanobiotechnol.*, 2019, **17**, 1–14.

18 Q. Han, Z. Wang, J. Xia, S. Chen, X. Zhang and M. Ding, Facile and tunable fabrication of Fe_3O_4/graphene oxide nanocomposites and their application in the magnetic solid-phase extraction of polycyclic aromatic hydrocarbons from environmental water samples, *Talanta*, 2012, **101**, 388–395.

19 S. Alilou, M. Amirzehni and P. A. Eslami, A simple fluorometric method for rapid screening of aflatoxins after their extraction by magnetic MOF-808/graphene oxide composite and their discrimination by HPLC, *Talanta*, 2021, **235**, 122709.

20 J. Ren, G. Liang, Y. Man, A. Li, X. Jin, Q. Liu and L. Pan, Aptamer-based fluorometric determination of Salmonella Typhimurium using Fe_3O_4 magnetic separation and CdTe quantum dots, *PLoS One*, 2019, **14**, 1–13.

21 R. Binaymotlagh, F. Hajareh Haghighi, F. Aboutalebi, S. Z. Mirahmadi-Zare, H. Hadadzadeh and M.-H. Nasr-Esfahani, Selective chemotherapy and imaging of colorectal and breast cancer cells by a modified MUC-1 aptamer conjugated to a poly(ethylene glycol)-dimethacrylate coated Fe_3O_4–AuNCs nanocomposite, *New J. Chem.*, 2019, **43**, 238–248.

22 F. Ghorbani and S. Kamari, Core–shell magnetic nanocomposite of Fe_3O_4@SiO_2@NH_2 as an efficient and highly recyclable adsorbent of methyl red dye from aqueous environments, *Environ. Technol. Innovation*, 2019, **14**, 100333.

23 X. X. Liang, X.-K. Ouyang, S. Wang, L.-Y. Yang, F. Huang, C. Ji and X. Chen, Efficient adsorption of Pb(II) from aqueous solutions using aminopropyltriethoxysilane-modified magnetic attapulgite@chitosan (APTS-Fe3O4/APT@CS) composite hydrogel beads, *Int. J. Biol. Macromol.*, 2019, **137**, 741–750.

24 G. Bayramoglu, V. C. Ozalp, M. Oztekin and M. Y. Arica, Rapid and label-free detection of Brucella melitensis in milk and milk products using an aptasensor, *Talanta*, 2019, **200**, 263–271.

25 J. Fu, H. Dong, Q. Zhao, S. Cheng, Y. Guo and X. Sun, Fabrication of refreshable aptasensor based on hydrophobic screen-printed carbon electrode interface, *Sci. Total Environ.*, 2020, **712**, 136410.

26 W. Wang, S. Liu, C. Li, Y. Wang and C. Yan, Dual-target recognition sandwich assay based on core-shell magnetic mesoporous silica nanoparticles for sensitive detection of breast cancer cells, *Talanta*, 2018, **182**, 306–313.

27 Y. Su, C. Shao, X. Huang, J. Qi, R. Ge, H. Guan and Z. Lin, Extraction and detection of bisphenol A in human serum and urine by aptamer-functionalized magnetic nanoparticles, *Anal. Bioanal. Chem.*, 2018, **410**, 1885–1891.

28 N. Yadav, A. Singh and M. Kaushik, Synthesis and characterization of hydrothermally synthesized superparamagnetic APTS–$ZnFe_2O_4$ nanoparticles: DNA binding studies for exploring biomedical applications, *Chem. Pap.*, 2020, **74**, 1177–1188.

29 M. H. Iha, C. B. Barbosa, R. M. D. Favaro and M. W. Trucksess, Chromatographic method for the determination of aflatoxin M1 in cheese, yogurt, and dairy beverages, *J. AOAC Int.*, 2011, **94**, 1513–1518.

30 Y. Zhao, Y.-C. Yuan, X.-L. Bai, Y.-M. Liu, G.-F. Wu, F.-S. Yang and X. Liao, Multi-mycotoxins analysis in liquid milk by UHPLC-Q-Exactive HRMS after magnetic solid-phase extraction based on PEGylated multi-walled carbon nanotubes, *Food Chemistry*, 2020, **305**, 125429.

31 H. Xu, J. Sun, H. Wang, Y. Zhang and X. Sun, Adsorption of aflatoxins and ochratoxins in edible vegetable oils with dopamine-coated magnetic multi-walled carbon nanotubes, *Food Chemistry*, 2021, **365**, 130409.

32 X. Wu, X. Zhang, Y. Yang, Y. Liu and X. Chen, Development of a deep eutectic solvent-based matrix solid phase dispersion methodology for the determination of aflatoxins in crops, *Food Chemistry*, 2019, **291**, 239–244.

33 Q. Li, L. Jiang, H. Zhang, M. Wei, C. Chu and J. Yan, Modified Magnetic Nanoparticle-Based Solid-Phase Extraction for the Determination of Trace Amounts of Aflatoxins B1 and B2 in Chinese Patent Medicines: The Use of Fupuganmao Granules as a Case Study, *J. AOAC Int.*, 2019, **102**, 761–766.

34 Y. Jia, G. Zhou, P. Liu, Z. Li and B. Yu, Recent Development of Aptamer Sensors for the Quantification of Aflatoxin B1, *Appl. Sci.*, 2019, **9**, 2364.

35 Y. Dong, B. Wen, Y. Chen, P. Cao and C. Zhang, Autoclave-free facile approach to the synthesis of highly tunable nanocrystal clusters for magnetic responsive photonic crystals, *RSC Adv.*, 2016, **6**, 64434–64440.

36 X. Zhang, H. Niu, Y. Pan, Y. Shi and Y. Cai, Modifying the surface of Fe3O4/SiO2 magnetic nanoparticles with C-18/NH_2 mixed group to get an efficient sorbent for anionic organic pollutants, *J. Colloid Interface Sci.*, 2011, **362**, 107–112.

37 F. Liu, X. Yang, X. Wu, X. Xi, H. Gao, S. Zhang, W. Zhou and R. Lu, A dispersive magnetic solid phase microextraction based on ionic liquid-coated and cyclodextrin-functionalized magnetic core dendrimer nanocomposites for the determination of pyrethroids in juice samples, *Food Chem.*, 2018, **268**, 485–491.

38 A. Pietri, S. Rastelli, A. Mulazzi and T. Bertuzzi, Aflatoxins and ochratoxin A in dried chestnuts and chestnut flour produced in Italy, *Food Control*, 2012, **25**, 601–606.

39 R. Luo, X. Zhou, Y. Chen, S. Tuo, F. Jiang, X. Niu, F. Pan and H. Wang, Lysozyme Aptamer-Functionalized Magnetic Nanoparticles for the Purification of Lysozyme from Chicken Egg White, *Foods*, 2019, **8**, 67–80.